Deep-Sea Research II 104 (2014) 134–144

Contents lists available at ScienceDirect

Deep-Sea Research II

journal homepage: www.elsevier.com/locate/dsr2

Recent sediment transport and deposition in the Cap-Ferret Canyon, South-East margin of Bay of Biscay

Sabine Schmidt [a,*], Hélène Howa [b], Amy Diallo [a], Jacobo Martín [c], Michel Cremer [a], Pauline Duros [b], Christophe Fontanier [b], Bruno Deflandre [d], Edouard Metzger [b], Thierry Mulder [d]

[a] CNRS, EPOC, UMR 5805, F-33400 Talence, France
[b] UMR CNRS 6112 LPGN-BIAF, Laboratoire des Bio-Indicateurs Actuels et Fossiles, LUNAM Université, Université d'Angers, 2 Boulevard Lavoisier, 49045 Angers Cedex, France
[c] Instituto de Ciencias del Mar (CSIC), Paseo Marítimo de la Barceloneta 37-49, 08803 Barcelona, Spain
[d] Université Bordeaux, EPOC, UMR 5805, F-33400 Talence, France

ARTICLE INFO

Available online 19 June 2013

Keywords:
Cap-Ferret Canyon
Bay of Biscay
^{210}Pb
^{234}Th
Sediment transport
Particulate flux
Sedimentation
Bioturbation

ABSTRACT

The Cap-Ferret Canyon (CFC), a major morphologic feature of the eastern margin of the Bay of Biscay, occupies a deep structural depression that opens about 60 km southwest of the Gironde Estuary. Detailed depth profiles of the particle-reactive radionuclides ^{234}Th and ^{210}Pb in interface sediments were used to characterise the present sedimentation (bioturbation, sediment mass accumulation, and focusing) in the CFC region. Two bathymetric transects were sampled along the CFC axis and the southern adjacent margin. Particle fluxes were recorded from the nearby Landes Plateau by means of sediment traps in 2006 and 2007. This dataset provides a new and comprehensive view of particulate matter transfer in the Cap-Ferret Canyon region, through a direct comparison of the canyon with the adjacent southern margin. Radionuclide profiles (^{234}Th and ^{210}Pb) and mass fluxes demonstrate that significant particle dynamics occur on the SE Aquitanian margin in comparison with nearby margins. The results also suggest show three distinct areas in terms of sedimentary activity. In the upper canyon ($<$ 500 m), there is little net sediment accumulation, suggesting a by-pass area. Sediment focusing is apparent at the middle canyon (500–1500 m), that therefore acts as a depocenter for particles from the shelf and the upper canyon. The lower canyon ($>$ 2000 m) can be considered inactive at annual or decadal scales. In contrast with the slow and continuous accumulation of relatively fresh material that characterises the middle canyon, the lower canyon receives pulses of sediment via gravity flows on longer time scales. At decadal scale, the CFC can be considered as a relatively quiescent canyon. The disconnection of the CFC from major sources of sediment delivery seems to limit its efficiency in particle transfer from coastal areas to the adjacent ocean basin.

1. Introduction

Submarine canyons are spectacular topographic features that are usually presented as natural conduits for the transfer of particulate matter from the shelf to the deep ocean on both passive and active continental margins (Carson et al., 1986; Gardner, 1989; Palanques et al., 2005; De Leo et al., 2010). Modern sedimentation rates have been found to be substantially higher in some submarine canyons than on the adjacent open slopes at similar depths (Carpenter et al., 1982; de Stigter et al., 2007; Mas et al., 2010). Large accumulations of sediment and detritus have been reported on the floors of canyons in different parts of the word (McHugh et al., 1992). Substantial amounts of these particles are not produced locally within the canyon, but transported from shallow coastal areas typically enriched in nutrients (Mullenbach and Nittrouer, 2000; Puig et al., 2003; Kao et al., 2006; Tesi et al., 2008; Pasqual et al., 2011). Thus, the chanelling of particulate transport within canyons gives rise to high planktonic and benthic production (Stefanescu et al., 1994; Vetter, 1994; Cunha et al., 2011; Hunter et al., 2013).

In spite of numerous studies conducted in submarine canyons around the world, the mechanisms governing the present-day transfer of particulate matter through submarine canyons, as well as the temporal scales involved, are not fully understood at present. This knowledge is important to understand why canyons

* Correspondence to: UMR 5805 EPOC, Université Bordeaux 1, Avenue des Facultés, 33405 Talence Cedex, France. Tel.: +33 540 00 33 15; fax: +33 540 00 33 16.
E-mail address: s.schmidt@epoc.u-bordeaux1.fr (S. Schmidt).

0967-0645/$ - see front matter © 2013 Elsevier Ltd. All rights reserved.
http://dx.doi.org/10.1016/j.dsr2.2013.06.004

are "hot spots" for biological activity, and how changes in particle supply (quality and intensity) could affect canyon ecosystems and associated productivity and biodiversity. The question is relevant as submarine canyons are extremely frequent features that incise into continental shelves and slopes of all continental margins. Harris and Whiteway (2011) have recently published the first global inventory of large submarine canyons, identifying a total of 5849 separate canyons in the world's oceans.

In the North-East Atlantic, the Bay of Biscay is bordered, from north to south, by the Celtic, Armorican, Aquitanian and North-Iberian margins, and cut by almost 35 submarine canyons (Reid and Hamilton, 1990; Bourillet et al., 2007; Mulder et al., 2012; Hunter et al., 2013, and references herein). The Aquitanian continental margin is constituted by a sedimentary basinward prograding prism over the marginal Landes Plateau. Two main canyons, the Cap-Ferret Canyon (CFC) and the Capbreton Canyon, have contributed to the construction of a single elongated deep-sea turbidite system, the Cap-Ferret system (Cremer et al., 1985; Fig. 1). The Cap-Ferret Canyon is a deep structural depression that opens off a 60 km wide shelf, and where an important drainage network converges from multiple incised channels. Southward, the Capbreton Canyon forms a deep and narrow E–W incision that begins 200 m from the shoreline and deepens regularly over 270 km down to the junction at 3400 m water depth with the S–N directed Santander Canyon, before merging 75 km further north with the CFC (Fig. 1).

The objective of this work is to characterise the present-day sediment transport and deposition within CFC using a multi-tracer approach. We report here detailed depth profiles of the particle-reactive radionuclides ^{234}Th ($T_{1/2}$=24.1 days) and ^{210}Pb ($T_{1/2}$=22.3 years) in interface sediments collected from 151 to 3168 m depth in the CFC region during the LEVIATHAN cruise (June, 2009). Two bathymetric transects were sampled, along the canyon axis and the southern adjacent margin. We present also downward particulate mass fluxes recorded, by means of sediment traps, in the nearby Landes Plateau between 2006 and 2007. Results of a first investigation of the CFC conducted in 1990 (ECOFER—ECOsystème du canyon de cap-FERet; Heussner et al., 1999) are also included. This dataset is discussed in order to compare the present sedimentation framework (bioturbation, sediment mass accumulation, and focusing) of the CFC and of the adjacent open slope and to define a conceptual framework of the sedimentary activity along the CFC. Based on a comparison with other canyons, we suggest the "Type II" canyon category, as defined by Jobe et al. (2011), to be subdivided into at least two classes.

2. Materials and methods

2.1. Settling particles in the water column

During the ANR-FORCLIM programme, a long-term mooring equipped with two sediment traps (PPS5 TECHNICAP; sampling area 1 m^2) was deployed at the deepest station 6′, on the Landes Plateau (southeast Aquitanian margin) (Fig. 1, Table 1). Settling particles were sampled at two water depths, 800 m and 1700 m respectively, over a 17-month period, from June 22, 2006, to November 23, 2007. Details on moorings, sample processing and data are given by Schmidt et al. (2009) and Kuhnt et al. (2013). Station 6′ (44°33′N, 2°45′W, 2000 m water depth) is also labelled WH in previous works on the Aquitanian margin; the label 6′ is preferred in this work for coherence with the notation of the other sites on the slope transect. During ECOFER, two trap moorings were also deployed, but in the canyon axis, at 2300 and 3000 m water depth, for 14 months from June 1990 to August 1991. Details on moorings and sample processing are given by Heussner et al. (1999).

2.2. Interface sediment

Our investigation deals with interface sediments obtained in the CFC and on the nearby southern margin, the Aquitanian margin down to the Landes Plateau (Fig. 1; Table 2). During the LEVIATHAN cruise (June 2009), two bathymetric transects were sampled between 153 and 3168 m water depth using a multicorer (Oktopus, MUC 8/100) to ensure a good recovery of the water–sediment

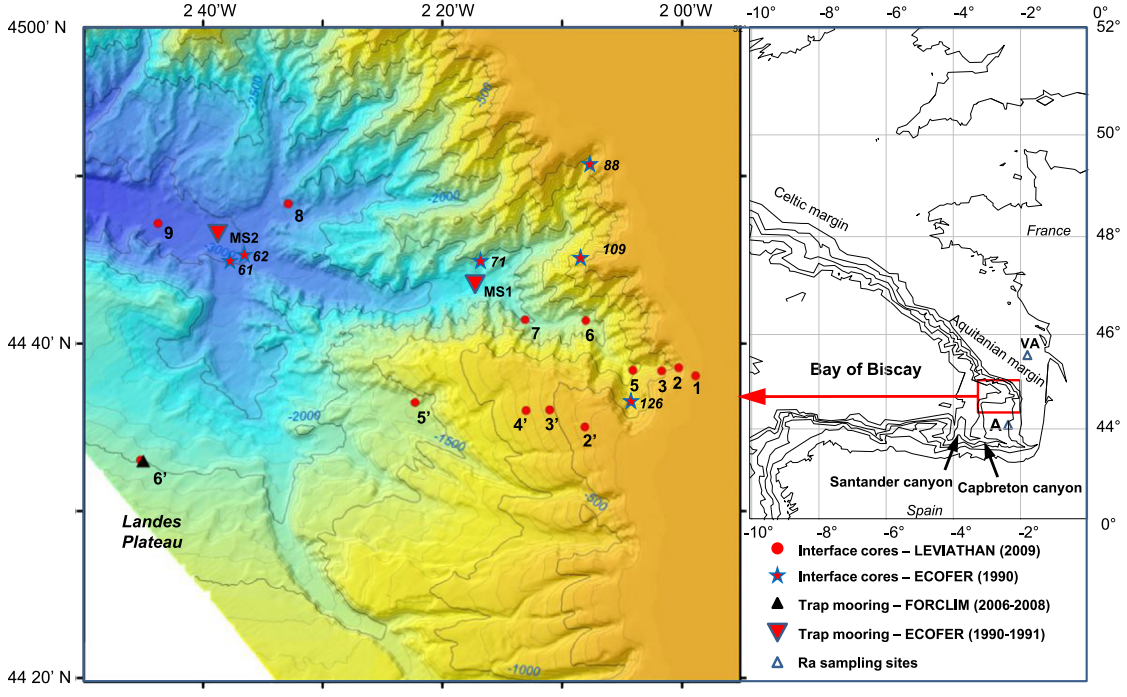

Fig. 1. Enlarged image of the Cap-Ferret Canyon in the S-E Bay of Biscay showing the location of the multicores collected at various depths in the canyon area and along a southern adjacent transect on the Aquitanian margin. Locations of trap moorings and sampling sites of dissolved ^{226}Ra are also indicated.

Table 1
Location, water column depth and sampling year of the long-term moorings; depth of the trap; mean annual mass flux; ^{210}Pb particulate flux (F) and ^{210}Pb$_{xs}$ flux/^{210}Pb annual production ratio (F/P).

Site	Latitude (°N)	Longitude (°W)	Water column depth (m)	Sampling year	Trap depth (m)	Total mass flux (mg cm^{-2} yr^{-1})	^{210}Pb$_{xs}$	
							F (mBq cm^{-2} yr^{-1})	F/P
Cap-Ferret canyon								
MS1*	44°44′	2°18′	2300	1990–1991	380	18.2*	34.0*	2.9
					1350	28.1*	49.2*	3.0
					1900	43.7*	82.2*	4.3
					2250	53.7*	101.7*	5.0
MS2*	44°47′	2°38′	3000	1990–1991	1900	11.9*	29.2*	1.5
					2950	16.7*	49.3*	2.1
Southern margin (Plateau des Landes)								
6′	44°33′	2°45′	2000	2006–2007	800	2.7	8.0	0.7
					1700	7.0	19.7	1.2

*: Traps and data from the ECOFER experiment (Heussner et al., 1999; Radakovitch and Heussner, 1999).

Table 2
Location, depth and sampling year of the cores; mean grain size of the layer 5-6 cm; information derived from seabed ^{210}Pb$_{xs}$ profiles: mixed layer thickness (ML), sedimentation and mass accumulation rates (SAR, MAR), ^{210}Pb particulate flux (F) and ^{210}Pb$_{xs}$ flux/^{210}Pb annual production ratio (F/P); surficial ^{232}Th activity; information derived from seabed ^{234}Th$_{xs}$ profiles: ^{234}Th inventory (I) and bioturbation rate (D_b).

Site	Latitude (°N)	Longitude (°W)	Depth (m)	Sampling year	Grain size (μm)	^{210}Pb$_{xs}$					^{232}Th (mBq g^{-1})	^{234}Th$_{xs}$	
						ML (cm)	SAR (cm yr^{-1})	MAR (mg cm^{-2} yr^{-1})	F (mBq cm^{-2} yr^{-1})	F/P		I (mBq cm^{-2})	D_b (cm^2 yr^{-1})
Cap-Ferret canyon													
1	44°38′079	1°58′852	151	2009	124	5	0.140	219	37.3	3.5	21	99	0.8
2	44°38′566	2°00′274	353	2009	17	6	0.084	130	67.0	5.8	25	50	0.4
KTB88 *			445	2000			0.280*	230	86.5*	7.1			
3	44°38′371	2°01′688	535	2009	14	3	0.370	293	128.1	10.3	56	107	n.d.
KTB126 *			750	2000			0.370*						
5	44°38′422	2°04′124	1035	2009	12	4	0.288	214	196.4	13.2	54	173	68.7
6	44°41′374	2°08′036	1695	2009	12	2–3	0.263	211	165.9	9.3	60	139	0.2
7	44°41′424	2°13′111	2050	2009	12	1–2	0.138	83	110.3	5.6	54	111	1.4
KTB71 *			2300	2000			0.200*	150	55.8*	2.7			
8	44°48′348	2°32′888	2890	2009	9	1	0.082	41	45.8	1.9	50	63	3.5
KTB62 *			2985	2000			0.040*	60	43.0*	1.8			
KTB61 *			2985	2000			0.030	30	28.2	1.2			
9	44°47′167	2°43′747	3168	2009	9	< 1	0.099	72	58.2	2.3	64	40	< 0.1
Interfluve													
KTB109 *			880	2000			0.140*	120	80.0*	5.7			
Southern margin (Plateau des Landes)													
2′	44°35′027	2°08′114	329	2009	44	7	0.290	409	43.3	3.8	42	35	0.3
3′	44°36′032	2°11′048	534	2009	36	1	0.111	152	20.6	1.7	54	129	0.2
4′	44°41′990	2°13′017	1010	2009	10	1–2	0.084	59	40.3	2.7	56	118	1.1
5′	44°36′481	2°22′306	1619	2009	9	1	0.067	45	40.2	2.3	54	58	0.4
6′	44°33′036	2°45′217	2078	2009	7	1–2	0.070	51	25.1	1.3	67	10	0.1

*: Cores and data from ECOFER cruise (Radakovitch and Heussner, 1999).

interface. Immediately after core retrieval, tubes (inner diameter 9.5 cm) were carefully extruded and sliced at 0.5 cm intervals from 0 to 4 cm, and at 1 cm intervals below that depth.

In the laboratory, dry bulk density (DBD) was measured by determining the weight after drying (60 °C) of a known volume of wet sediment. ^{234}Th, ^{238}U, ^{210}Pb, ^{226}Ra and ^{232}Th activities were measured on 2.5–5 g of dried sediment using a semi-planar germanium detector (EGSP 2200-25-R, EURYSIS Mesures) (Schmidt et al., 2009). Within 6 weeks after sampling, because of the rapid decay of ^{234}Th, the uppermost sediment layers of each core were measured by γ-counting, until a rather constant ^{234}Th activity was reached. After 3–4 months, a second determination was performed to determine the supported ^{234}Th activities. The standards used for the calibration of the γ detector are RGU and RGTh gamma standards from IAEA. Errors on radionuclide activities are based on 1 standard deviation counting statistics. Excess ^{234}Th (^{234}Th$_{xs}$) and ^{210}Pb (^{210}Pb$_{xs}$) data were calculated by subtracting the activity supported by their parent isotopes, ^{238}U and ^{226}Ra respectively, from the total activity in the sediment, and then by correcting ^{234}Th values for radioactive decay that occurred between sample collection and counting (this correction is not necessary for ^{210}Pb due to its longer half-life and the short time between sampling and analysis). Errors on ^{234}Th$_{xs}$ and ^{210}Pb$_{xs}$ are calculated by propagation of errors in the corresponding pair, ^{234}Th and ^{238}U, or ^{210}Pb and ^{226}Ra. Grain size analyses on a wet sediment aliquot (layer 5–6 cm of each core) were performed with a Malvern® Laser diffraction particle sizer.

2.3. Bioturbation rates

Sedimentation and mixing rates are generally determined by means of tracers, which reach the seafloor in association with

particles settling through the water column (Nittrouer et al., 1984). For seasonal time scales, an appropriate tracer is ^{234}Th, a natural decay-product of ^{238}U (Aller and Cochran, 1976). Taking into account its very short half-life ($T_{½}$=24.1 days) and sedimentation rates usually encountered in continental slopes and shelves (far less than 1 cm yr^{-1}), $^{234}Th_{xs}$ should be present only at the water–sediment interface. ^{234}Th penetration to variable depths indicates efficient mixing of the upper sediments, usually by bioturbation. The simplest way to derive bioturbation rates (D_b) from radionuclide profiles is to assume bioturbation as a diffusive process occurring at a constant rate within a surface mixed layer under steady state (Schmidt et al., 2001). These simplifications allow the determination of bioturbation rates from a simple plot of radionuclide activity as a function of depth z (cm), using

$$[^{234}Th_{xs}]_z = [^{234}Th_{xs}]_0 \exp\left(-z\sqrt{\frac{\lambda}{D_b}}\right), \quad (1)$$

where $[^{234}Th_{xs}]_0$ and $[^{234}Th_{xs}]_z$ are the activities (mBq g^{-1}) of excess ^{234}Th at the water–sediment interface, z the depth, λ the decay constant of the nuclide, and D_b the bioturbation rate. We present ^{234}Th-derived bioturbation rates and inventories as an indication of particle input over the last few months. Such bioturbation rates must be considered as an instantaneous signal (Aller and DeMaster, 1984; Schmidt et al., 2001).

2.4. Sedimentation and mass accumulation rates, focusing

For decadal to century time scales, the classically-used tracer is ^{210}Pb, a natural decay-product of ^{226}Ra, with a half-life of 22.3 years (Appleby and Oldfield (1992), and references herein). The ^{210}Pb method is based on the measurement of the excess or unsupported activity of ^{210}Pb ($^{210}Pb_{xs}$) which is incorporated rapidly into the sediment from atmospheric fallout and water column scavenging, due to the strong affinity of ^{210}Pb for particulate matter. Once incorporated into the sediment, unsupported ^{210}Pb decays with depth, equivalent to time, in the sediment column according to its known half-life. Several models have been developed to calculate an age or accumulation rate (Sanchez-Cabeza and Ruiz-Fernández, 2012, among others): CIC (constant initial concentration); CSR (constant rate of supply); and CFCS (constant flux-constant sedimentation). In order to compare this work with a former investigation of the CFC conducted in 1990, we have chosen to apply the same model, the CFCS model, which is commonly used in marine sediments. Under the two assumptions of the CFCS method, constant flux and constant sediment accumulation rates (Robbins and Edgington, 1975), sediment accumulation rate can be derived from the decrease of $^{210}Pb_{xs}$ activities with depth considering the following relation:

$$[^{210}Pb_{xs}]_z = [^{210}Pb_{xs}]_0 \exp\left(-z\frac{\lambda}{SAR}\right), \quad (2)$$

where $[^{210}Pb_{xs}]_0$ and $[^{210}Pb_{xs}]_z$ are the activities of excess ^{210}Pb at the water–sediment interface, or the base of the mixed layer, z the depth, λ the decay constant of the nuclide, and SAR the sediment accumulation rate. In this model, the compaction and bioturbation effects are not taken into account, and calculated SAR correspond to maximum values. An alternative method is to plot the regression of $^{210}Pb_{xs}$ against cumulative mass to calculate a mass accumulation rate (MAR), which integrates the compaction effect.

A complementary way to characterise deposition fluxes is to compare the annual seabed $^{210}Pb_{xs}$ flux (F) and the predicted ^{210}Pb flux (P) using the focusing ratio (F/P). Values of $F/P > 1$ suggest focusing or lateral input of ^{210}Pb to the considered site (Muhammad et al., 2008). In the open ocean, the sources of ^{210}Pb are atmospheric fallout of ^{210}Pb to surface waters and its production in the water column from decay of ^{226}Ra (Cochran et al., 1990). For atmospheric deposition, we use the value of 8.5 ± 1.3 mBq cm^{-2} yr^{-1} (Schmidt et al., 2009). The production rate from the water column was calculated using the profiles of ^{226}Ra at site 6′ (water depth=2078 m), and at two sites on the Landes Plateau (A, water depth=1000 m) and on the shelf (V4, water depth=67 m, see Fig. 1). To determine dissolved ^{226}Ra activities, 20 L samples were recovered from different depths in the water column by draining seawater from Niskin bottles of a CTD rosette. On board, ^{226}Ra was immediately co-precipitated with $BaSO_4$. In the lab, ^{226}Ra activities were measured by γ-counting (Schmidt and Reyss, 1996). A very low-background, high-efficiency well-type germanium detector (Ge volume of 260 cm^3, low-noise Al and Cu components) equipped with a Cryo-Cycle (CANBERRA) was used in the underground laboratory of the EPOC laboratory. ^{226}Ra activities present slight differences between the three stations, with a mean value of 1.4 ± 0.2 mBq m^{-3} (Fig. 2). The increase in activities toward the seafloor is explained by diffusion of radium from bottom sediments (Cochran, 1980).

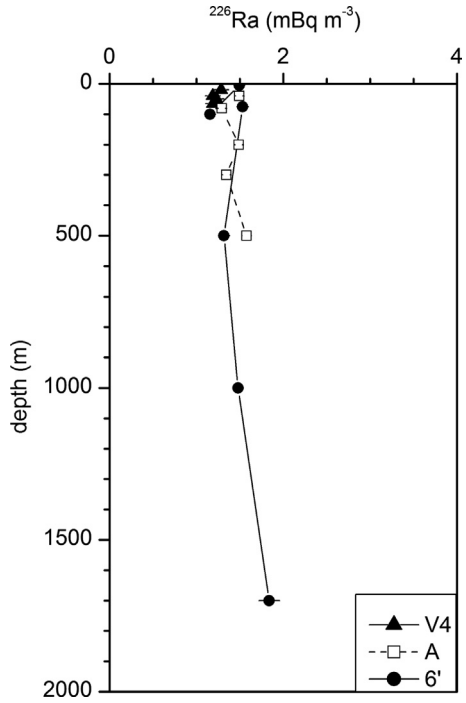

Fig. 2. Profiles of ^{226}Ra with depth of the water column on the shelf (V4, water depth=67 m), the middle slope (A, water depth=1000 m) and Plateau des Landes (6′, water depth=2078 m) (S-E Bay of Biscay).

Predicted ^{210}Pb fluxes, based on these ^{226}Ra profiles, are comprised between 10.7 and 24.8 mBq cm^{-2} yr^{-1}, increasing with water column depth. The annual $^{210}Pb_{xs}$ flux (F, mBq cm^{-2} yr^{-1}) is calculated from the seabed inventory as

$$F = \lambda(\sum A_i \, DBD_i \, dz),$$

where A_i (mBq g^{-1}) is the excess ^{210}Pb of the sampled layer i, and dz (cm) and DBD_i (g cm^{-3}) are respectively the thickness (0.5 or 1 cm) and the dry bulk density of this layer.

3. Results

3.1. Seabed $^{234}Th_{xs}$ profiles

Thorium data indicate the occurrence of excess ^{234}Th in the top of all the studied cores (Fig. 3). Such an occurrence of ^{234}Th demonstrates the presence of freshly deposited particles. Sedimentary

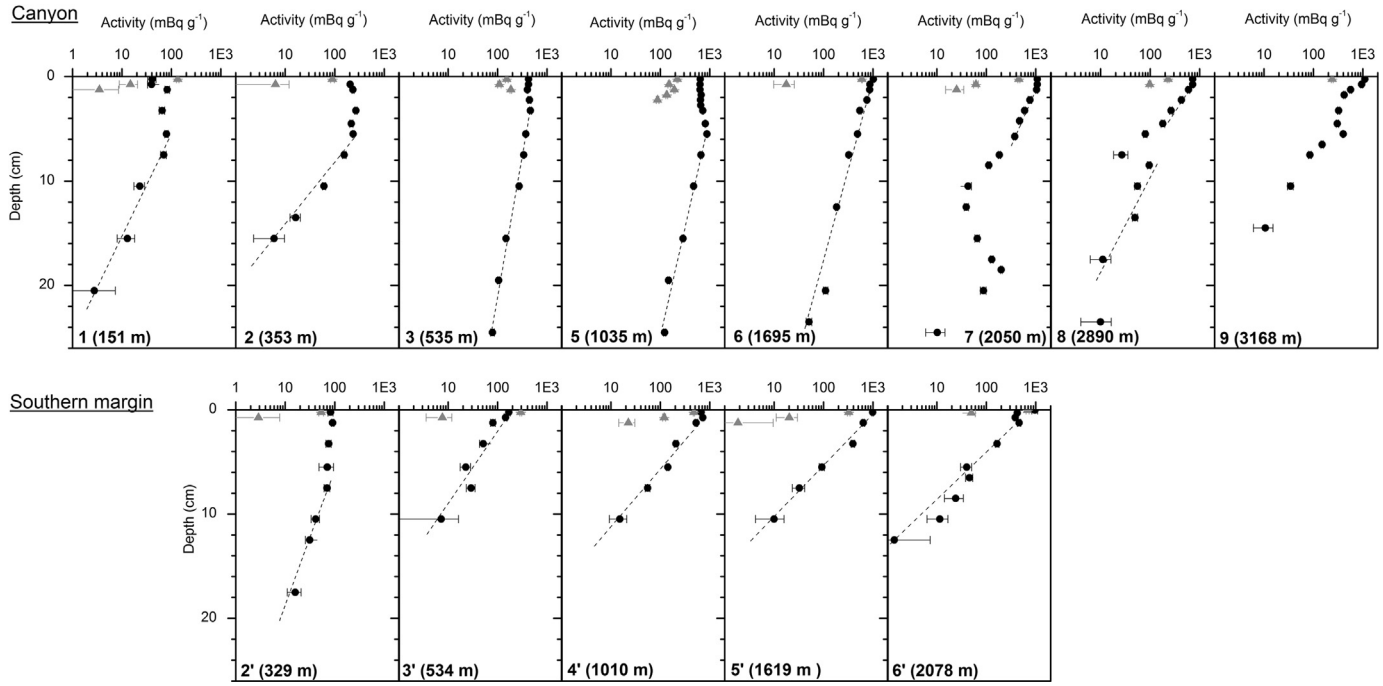

Fig. 3. $^{234}Th_{xs}$ (grey triangles) and $^{210}Pb_{xs}$ (black dots) profiles measured on the cores from the Cap-Ferret Canyon (upper panel) and from the southern margin (lower panel). The profiles have been plotted from left to right with increasing water column depth. Error bars on radionuclide profiles correspond to 1 SD. Dashed lines show the regression line used to calculate SAR.

$^{234}Th_{xs}$ profiles in the canyon and on the open slope show variable penetration depths, from 0.5 to about 4 cm, which reveal contrasted mixing efficiency. Five profiles were collected outside the canyon, from 329 to 2078 m water depth across the southern margin (Fig. 3; lower panel): $^{234}Th_{xs}$ of all these profiles disappears very rapidly within the first centimetre. Margin profiles present always equivalent or lower $^{234}Th_{xs}$ activities, compared to the canyon profiles at similar depth. Inventories present also marked differences among sites, between 10 and 173 mBq cm^{-2}, the lowest values being recorded in the deepest core of the open slope transect (station 6′, water depth = 2068 m). Except for sites 3 (water depth = 535 m) and 5 (water depth = 1035 m) in the upper canyon, bioturbation rates (0.1–3.5 cm^2 yr^{-1}) are in the range of reported values for margin environments (Legeleux et al., 1994; Schmidt et al., 2002).

3.2. Seabed $^{210}Pb_{xs}$ profiles

In the CFC, surface excess ^{210}Pb activities range from 41 to 1101 mBq g^{-1}. Profiles of $^{210}Pb_{xs}$ present a well-developed mixed layer in the upper canyon (cores 1–3, and 5), that becomes negligible for cores at water depths > 1500 m (Table 2; Fig. 3). Deeper in the sediment $^{210}Pb_{xs}$ profiles follow an exponential decrease in most of the sampled canyon stations. In cores 3 (water depth = 535 m), 5 (water depth = 1035 m), and 6 (water depth = 1695 m), ^{210}Pb at the basis of the core (typically the layer at 24–26 cm) is still far from the equilibrium value with its progenitor, ^{226}Ra. In the other cores of the canyon (sites 1, 2, and 7–9), $^{210}Pb_{xs}$ activities reach supported activities at depths ranging between 15 and 25 cm. The $^{210}Pb_{xs}$ profile in core 7 (water depth = 2050 m) presents a peculiar feature, with a layer between 8 and 18 cm exhibiting lower activities, by comparison with the surrounding layers. In the deep reaches of the canyon, cores 8 (water depth = 2809 m) and 9 (water depth = 3168 m) show a similar feature, although less expressed and located in the uppermost part of the core. Such layers with low to very low ^{210}Pb activities suggest mixing with older eroded sediments and/or dilution with coarse sediment.

During the ECOFER experiment, interface sediments were also sampled at six sites (Fig. 1): it is noticeable that the same pattern (a layer presenting a marked decrease in $^{210}Pb_{xs}$ activities) is present in $^{210}Pb_{xs}$ profiles of three cores (KTB126, 71 and 61 at 720, 2300 and 3000 m water depths, respectively) (Radakovitch and Heussner, 1999).

On the adjacent slope (Fig. 3, lower panel), surface excess ^{210}Pb activities range from 82 to 990 mBq g^{-1}. Only the shallowest site (2′; water depth = 329 m) presents a mixed layer, about 7–8 cm thick. Then, $^{210}Pb_{xs}$ activities present an exponential decrease to reach supported levels at about 20 cm for site 2′ and 10 cm for site 6′ (water depth = 2078 m).

In the canyon, sedimentation and mass accumulation rates range between 0.08 and 0.37 cm yr^{-1}, and between 41 and 293 mg cm^{-2} yr^{-1}, respectively (Table 2). These values are consistent with the few values obtained during the ECOFER cruise. On the open adjacent slope, SAR and MAR are not significantly different: 0.08–0.29 cm y^{-1} and 45–409 mg cm^{-2} yr^{-1}.

3.3. Sediment ancillary data

Mean grain size ranges between 7 and 124 μm (Table 2). The 5–6 cm layer of the shallowest station 1 (water depth = 151 m) is dominated by sand. But grain sizes decrease rapidly with water depth to reach values < 10 μm, characteristic of fine silt, on both transects (Fig. 4). In order to explain the low $^{210}Pb_{xs}$ layers in the deep canyon (sites 7–9), corresponding layers were also analysed for grain size (data not shown). There is no obvious trend, only a slight increase in D_{90} that could indicate some sediment winnowing. These low $^{210}Pb_{xs}$-layers are not explained by a dilution by coarse material, and may indicate a massive input of older material.

The long-lived and naturally occurring ^{232}Th is usually associated with the detrital fraction (Van der Klooster et al., 2011), therefore activity changes can be an indication of different lithological sources or proportions. ^{232}Th activities range between 21 and 67 mBq g^{-1}, the lowest values are associated with the

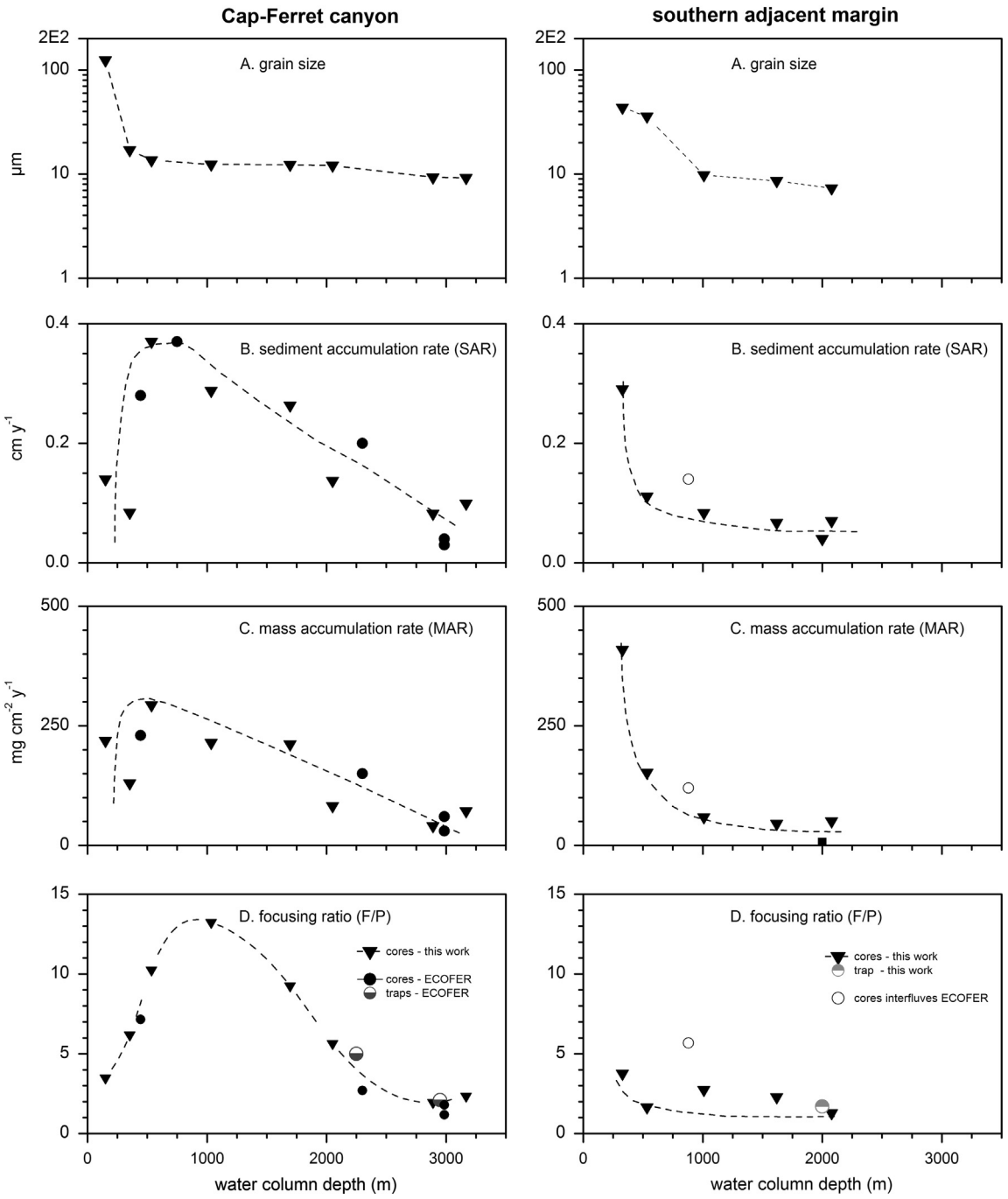

Fig. 4. Mean grain size of the topmost 5–6 cm of sediment cores (A), sediment (B) and mass (C) accumulation rates, and focusing ratio (D) against water depths of the stations along the CFC and the southern adjacent margin.

coarsest sediment of site 1 (Table 2). As for mean grain size, ^{232}Th values reach rapidly homogeneous and similar values on both transects. The enhanced activities in depth are consistent with the silty nature of sediment.

3.4. Sediment traps

The total particulate mass flux, registered by two sediment traps moored at site 6′ (water depth=2078 m) on the Landes Plateau, ranged from 0.6 to 13.6 mg cm^{-2} yr^{-1} at 800-m-depth and from 1.3 to 33.4 mg cm^{-2} yr^{-1} at 1700-m-depth (data not shown; see Schmidt et al. (2009) and Kuhnt et al. (2013) for details). Over the 17-month period, mean-trapped particulate fluxes were 2.7 and 7.0 mg cm^{-2} yr^{-1} at 800-m and 1700-m water depth respectively (Table 1). Particulate flux was much higher in the deepest trap, close to the mass accumulation rates obtained in the underlying sediment (site 6′). Mean *F*/*P* ratios of trapped particles increase with depth from 0.7 at 800 m water depth to 1.2 at 1700 m water depth. *F*/*P* ratios of trapped particles in the deepest trap agree also with the recorded *F*/*P* in the deepest cores on both transects (Fig. 4).

During the ECOFER experiment, two mooring lines equipped with sediment traps were used to record particulate fluxes in the CFC axis at 2300 (MS1) and 3000 m (MS2) water depth. Mean particulate fluxes trapped 50 m above sea bottom were 53.7 and 16.7 mg cm^{-2} yr^{-1} respectively, with a marked decrease offshore.

Taken into account the following observations: (1) the deepest trap on the Landes Plateau was moored 300 m above the sea-bottom, (2) the obvious increase of mass flux with depth in the water column at site 6′ (Table 1), and (3) the different sampling periods (14-months from 1990 to 1991 for ECOFER; 17-months from 2006 to 2007 for FORCLIM), the difference in mean-trapped particulate fluxes on the Landes Plateau and in the deep canyon (MS2) is assumed to be negligible. We have also calculated *F*/*P* ratios of ECOFER traps (Table 1) to compare with the present work. The mean annual mass flux collected by traps never exceeded the highest mass accumulation rates recorded in interface sediment of the upper canyon (Tables 1 and 2).

4. Discussion

4.1. Present-day sediment deposition in the CFC and on the adjacent open slope

Sedimentation rates on the open slope of the Aquitanian margin are higher, at equivalent depths, than those observed on nearby margins to the north in the Goban Spur and Meriadzek areas (van Weering et al., 1998), and to the South on the Iberian margin (van Weering et al., 2002). In contrast to these neighbouring systems, that receive little sediment from land due to distance from the coastline or to low river discharge, the S.-E. Aquitanian margin receives notable sediment input, estimated to be about 3.7 Mt yr^{-1}, through the Gironde, the Adour and the small Pyrenean and Cantabrian mountainous rivers (Ruch et al., 1993; Maneux et al., 1999). Thereafter, different hydrological processes (eddies, tidal energy) are favourable to offshore transport and redistribution of particles on the Aquitanian margin (Pingree and Le Cann, 1995; de Madron et al., 1999; Kuhnt et al., 2013).

High $^{234}Th_{xs}$ inventories are the signature of a significant particle input within the last 100 days (Aller and DeMaster, 1984) whereas bioturbation rates have been shown to vary with organic carbon fluxes (Schmidt et al., 2002). When considering $^{234}Th_{xs}$ inventories and bioturbation rates with depth, both show enhanced values at stations 3 (water depth = 535 m) and 5 (water depth = 1035 m) in the middle reaches of the CFC (Table 2). This is associated with the lowest oxygen penetration depth recorded on the two transects (0.4 cm at station 5; Duros et al., 2013). The simultaneous occurrence of these three signals may indicate that a high, rapid sedimentation of fresh particles had occurred recently in the depth range between 500 and 1500 m in the canyon, probably in association with the downward settling of recent spring bloom production (LEVIATHAN cruise was performed during late June).

On a longer time scale, there are also differences in sediment deposition between the two transects (Fig. 4B and C). On the adjacent open slope, sediment accumulation rates decrease rapidly with increasing depth and distance from the shelf break, from 0.29 to 0.08 cm yr^{-1}. This trend is usually observed in margin sediments (Muhammad et al., 2008), and in particularly in NW European margins (Antia et al., 1999; van Weering et al., 1998, 2002; Schmidt et al., 2009).

In the canyon, accumulation rates present a more complex pattern (Fig. 4B and C). Three areas can be distinguished. The low sedimentation rates at water depth < 500 m indicate that the upper canyon is not a depocenter. The accumulation rate at station 2 (water depth = 353 m) is even lower than that at the open margin at a similar depth (Fig. 4). In the middle part of the CFC, at water depths between 500 and 1500 m, sediment accumulation rates are the highest, up to 0.37 cm yr^{-1}. In the lower part of the canyon, SAR decreases smoothly to < 0.1 cm yr^{-1} at 3168 m water depth. These sediment accumulation rates are not drastically different from those recorded on the Landes Plateau (water column depth = 2078 m). Sedimentation rates in the middle CFC are in the lowest range of values that could be observed in canyons. For example several centimeters per year have been reported in the thalweg (Mulder et al., 2001) or on a terrace of the nearby Capbreton Canyon (Gaudin, 2006; Gaudin et al., 2006) and in the Nazaré canyon (de Stigter et al., 2007).

Stations 7 (water depth = 2050 m), 8 (water depth = 2890 m) and 9 (water depth = 3168 m) all show a subsurface layer presenting lower $^{210}Pb_{xs}$ activities than those in overlying and underlying sediments. The upper limits of this layer are 8, 5 and 6 cm respectively. This could correspond to the supply of older particles detached from the shelf, the canyon head and the upper slope and transported by a sediment gravity flow that reached the lower part of the CFC about 60 years ago.

The annual seabed $^{210}Pb_{xs}$ flux to the predicted ^{210}Pb flux ratio (*F*/*P*) reproduces the same trends as those observed for sediment and mass accumulation rates (Table 2; Fig. 4). On the adjacent open slope, *F*/*P* decrease rapidly to low values (1–2) with increasing depth, while in the canyon *F*/*P* values show a wider range and a different evolution with depth. The highest values, > 10, are recorded in the middle canyon. In the lower canyon, there is a convergence of *F*/*P* to values ranging between 1.2 and 2.3 with no distinction in the canyon or on the open slope. The high *F*/*P* ratios in the middle canyon reveal an enrichment of seabed $^{210}Pb_{xs}$ with respect to vertical scavenging of in situ production; it is also reflected in the distribution of $^{234}Th_{xs}$. There is lower $^{234}Th_{xs}$, *F*/*P* and SAR in the upper canyon (stations 1 and 2, water depth = 151 and 353 m respectively) than in the middle canyon (stations 3, 5, 6, water depths comprised between 535 and 1695). This violation of the general decreasing trend of mass fluxes with distance to the shore, as observed in the open margin stations, speaks clearly of an apparent continuous transfer of mass from the upper to the middle canyon. In addition the high *F*/*P* and MAR indicate that sediment is also transported along the continental shelf and is captured by the canyon. It mixes with the material resuspended at the canyon head. All the particles settle rapidly down through the upper and middle parts of the canyon. Radioisotope fluxes in the lower canyon, at water depth > 1500 m are only slightly higher than values measured at comparable water depths on the open adjacent slope, indicating that sediment inputs are focused within the middle part of the canyon.

4.2. Settling fluxes of particulate matter in the CFC and on the adjacent open slope

Mean annual particulate fluxes recorded by the deepest trap of the different moorings in the canyon and on the adjacent margin present a good agreement with seabed mass accumulation rates (Table 1; Fig. 4D). Therefore, particulate fluxes recorded on annual time scale in the Cap-Ferret area are representative of long term accumulation trends. This constancy indicates that the steady sedimentation is not restricted to the Aquitanian margin but also applied to the CFC.

The comparison of downward particulate fluxes recorded at different sites confirms this assumption (Fig. 5). Considering the 16-year time lapse between the moorings ECOFER (1990–1991) and FORCLIM (2006–2007), the mean annual particulate fluxes could be considered as similar in the remote traps moored in the deep canyon (MS2, water depth = 3000 m) and on the Landes Plateau (6′, water depth = 2078 m). Although these traps were set at different depths, they were localised at the same distance (30 km) from the shelf break.

Particulate fluxes increase with depth in the water column whatever the considered mooring. However, whereas at bathymetry < 1500 m the three moorings show a similar increase in

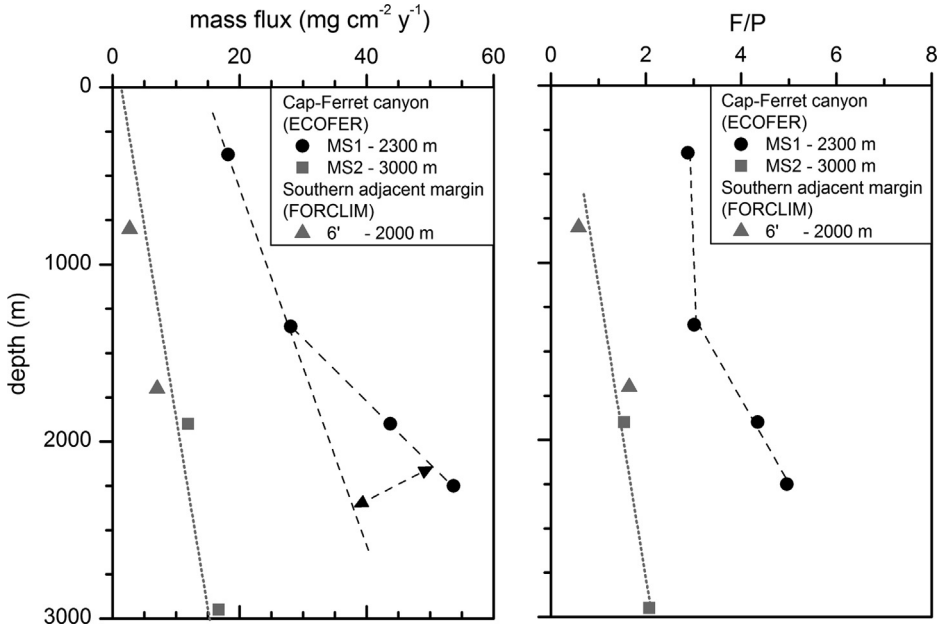

Fig. 5. Time-integrated average downward mass fluxes, measured by sediment traps deployed at different depths in the CFC (ECOFER, 1990–1991) and on the open adjacent margin (FORCLIM, 2006–2007).

mass flux with depth, MS1 (water depth = 2300 m) presents a distinct intensification of export in the deepest 500 m above seabed (Fig. 5). When extrapolating the increase observed in the upper waters, MS1 received at depth an excess of material of about 35 mg cm^{-2} yr^{-1}, by comparison with MS2. This could be explained by two parameters: the MS1 site is located at a location closer to the shelf break and at the confluence of two large gullies. There are also differences in trapped *F*/*P* ratios, with a large increase toward seabed in MS1, confirming a large contribution of lateral input. This effect is negligible in traps MS2 and 6′, as already observed in seabed sediments of the deepest locations (Fig. 4).

The decrease in particulate fluxes, trapped and seabed *F*/*P* ratios, and the reduction in sediment deposition with depth and distance from the shelf break, all these signals suggest that the particulate transfer is dominated by intermediate and bottom nepheloid layers propagating seaward (Ruch et al., 1993; de Madron et al., 1999). On the adjacent open slope, Kuhnt et al. (2013) have already concluded, using planktic foraminiferal tests and particulate mass fluxes, that the stratification of the water column and the evolution of midwater sediment plumes detaching from the shelf-break and upper continental slope affect downward particle flux dynamics. Possible energy sources for offshore transport of particles and consequent lateral advection at depth are hydrological structures such as eddies (Reverdin et al., 2013). Energy sources for sediment resuspension are tidal energy rays, which reach the shelf edge and upper continental slope of the south-eastern Bay of Biscay at a low angle (de Madron et al., 1999; Kuhnt et al., 2013).

Using ECOFER sediment trap data, Beaufort and Heussner (1999) have also showed that lateral transport of coccoliths resuspended from continental shelf and/or upper slope sediments seems to be the dominant transfer process to deep settings in the CFC. From the clear seasonal succession observed in the species composition, these authors have postulated that this deposition/resuspension/transport sequence is rapid (presumably less than a few months). Suykens et al. (2011) have also observed high resuspension of fresh and fine material at the shelf break in the Northern Bay of Biscay associated with a northward along slope current (Pingree and Le Cann, 1995).

4.3. Conceptual framework of the sedimentary activity in the CFC canyon

Fig. 4 illustrates the contrasting situations of across-margin sediment transport between the canyon and the open slope. While the margin presents the typical decreasing trend of sediment accumulation rates with distance to the shoreline and depth, this trend is visibly disrupted along the CFC, where at least three distinct areas can be identified in terms of their sedimentary status. The upper canyon (water depths < 500 m) is not a depocenter but rather a by-pass area where recent sediment inputs are balanced by sediment remobilization. This is supported by the lower accumulation rate and *F*/*P* and the higher grain size (possibly related to winnowing, suggesting high current speeds and resuspension at that part of the canyon) than those at the middle canyon (Fig. 4; Table 2). It is noteworthy that the accumulation rate at Station 2 (water depth = 353 m) is even lower than that at the open margin at a similar depth (Fig. 3). The upper canyon is hence considered a "by-pass" area where a substantial part of the sediment inputs do not accumulate but are advected elsewhere, most likely downslope towards the middle canyon.

The middle canyon acts as a depocenter on annual to decadal timescales, as illustrated by the high sediment accumulation rates and *F*/*P* recorded at water depths between 500 and 1500 m (Fig. 4). But the gravity flow imprinted in the lower canyon (Stations 7–9 in Fig. 3) testifies to episodic downcanyon flushing of the sediments accumulated in the middle canyon. This indicates that the middle canyon acts, on a longer timescale, as a temporary depocenter of sediment, including biogenic particles from the water column, nepheloid layers from the shelf and advection from the upper canyon.

In the lower canyon (water depths > 2000 m), the calculated annual sediment fluxes are similar to those at the open slope at similar depths hence this part of the canyon can be considered "inactive" at annual or decadal scales. Instead of receiving almost continuous inputs of relatively fresh material as the middle canyon, the lower canyon receives pulses of sediment via gravity flows on longer time scales. These short interface cores do not allow to calculate a "return period", but the fact that several

cores captured a substantial event from only ~60 years ago, is noteworthy.

4.4. Canyon category

The efficiency of a canyon in particle transfer is expected to be predicted on the basis of its geomorphological characteristics and its location compared to the adjacent shelf and the coastline, and a direct, or not, link with river systems. Jobe et al. (2011) recognise two main types of submarine canyons and associated depositional processes: "Type I" canyons deeply incise the shelf edge, resulting in narrow adjacent shelves, and are linked to areas of high coarse-grained sediment supply, generating erosive canyon morphologies, sand-rich fill, and large downslope submarine fans/aprons. These canyons are often connected to the dispersal of modern fluvial sediment (Mullenbach and Nittrouer, 2000; Mas et al., 2010; Huh et al., 2009; Puig et al., 2003). Resuspension of modern fluvial sediment on the shelf and advection over the canyon by alongshore currents and during storms cause large volumes of sediment to reach the head of the canyon (Mulder et al., 1998). Then an energetic process must trigger the mass transport of sediments previously stored in the canyon head to the deep canyon. Recent works illustrate the importance of storm-induced head-to-middle canyon transport (Martín et al., 2011; Mulder et al., 2001; Palanques et al., 2011).

"Type II" canyons do not incise the shelf edge and exhibit smooth, highly aggradational morphologies, mud-rich fill, and a lack of downslope fans/aprons. Type I canyons are dominated by erosive, sandy turbidity currents, sediment gravity flows and mass-wasting (de Stigter et al., 2007; Gaudin et al., 2006; Kao et al., 2006; Palanques et al., 2008; Bolliet et al., 2014), whereas Type II canyons are mainly sculpted by depositional processes related to hemipelagic deposition and dilute, sluggish turbidity (Hung et al., 2003; Jenner et al., 2007; Straub and Mohrig, 2009; Schmidt et al., 2010; Duros et al., submitted for publication).

Transposed to the Bay of Biscay, the two canyons that delimit the Aquitanian continental margin belong each to a different type. Located to the south, the Capbreton Canyon clearly comes within the Type I. The deepest submarine valley of the world (Shepard and Dill, 1966) beginning at only about 200 m off the French coastline, Capbreton Canyon follows regional tectonic directions related to the presently active Pyrenean thrust (Gaudin et al., 2006), and is considered as the main conduit for coast-to-abyss sedimentary transfers along the Aquitanian margin (Mulder et al., 2012, and references therein). On the contrary, the CFC falls within the Type II category. It is located at the shelf edge, at about 60 km apart from the large fluvio-estuarine system of the Gironde River. Our results show that particulate transfer does not appear intensified by comparison to the adjacent open slope, except in the middle canyon that acts as a natural trap due to its morphology. Therefore we suggest the type II canyons to be subdivided into at least two categories. First there are probably a large number of "dormant" canyons along the edges of the present continental shelves that have become presently inactive in terms of bulk sediment transport, since the sea-level rise has disconnected these systems from continental sediment sources (Reid and Hamilton, 1990; Zaragosi et al., 2000; Schmidt et al., 2010). These dormant canyons can be sporadically active during unpredictable and far-reaching events like exceptional storms, dense water cascading or earthquakes that efficiently transport sediment down-canyon (Ogston et al., 2008; Puig et al., 2008).

The second category corresponds to "quiescent" canyons, like the CFC. The head of such systems captures suspended sediments via intermediate and bottom nepheloid layers detached from the adjacent shelf or upper slope. In the Lisbon-Setubal and Cascais canyons, de Stigter et al. (2011) have shown that fine-grained predominantly lithogenic sediment accumulates in the upper reaches of these systems and that sediment deposited further down in the middle and lower reaches of canyons is essentially similar to the hemipelagic sediment found on the adjacent continental slope, indicating that down-canyon transport of sediment from the upper to the lower canyon is limited upstream. In Cascais Canyon sediment gravity flows transporting sediment down-canyon seem to have occurred only rarely during the last few centuries. In the CFC, the amazing coherence between the two dataset (ECOFER and LEVIATHAN cruises), considering the time interval between the experiments, demonstrates also the rather regular and calm sedimentation. This does not exclude rarer and violent downslope sediment transport, as suggested by subsurface layers of old (^{210}Pb-depleted) sediments observed in cores 7 (water depth = 2050 m), 8 (water depth = 2890 m) and 9 (water depth = 3168 m) from the lower part of the CFC. "Quiescent" canyons can be exceptionally active during extreme and unpredictable events such as centennial storms or high-magnitude earthquakes.

5. Conclusion

Sedimentary radionuclide profiles (^{234}Th and ^{210}Pb) have evidenced that significant contemporary particle dynamics take place on the SE Aquitanian margin in comparison with nearby margins, whereas the CFC experiences moderate and constant sedimentation, and thus could be considered as a quiescent canyon. The comparison of our data with the ECOFER data shows a striking similarity in mass fluxes in the deep reaches of the CFC, within a 16-year period. Short-lived events, like seasonal downward export of surface biological production, may leave a tiny imprint in the deposited layers, as revealed by the presence of ^{234}Th excess only at the water–sediment interface.

In CFC, focusing of fine sediment is confined to the middle canyon at about 500–1500 m and likely related to intermediate and bottom nepheloid layers detached from the shelf and the upper slope. This is reflected in the high $^{210}Pb_{xs}$ fluxes and F/P and the presence of $^{234}Th_{xs}$. In the upper canyon (water depths < 500 m), the results suggest by-passing of sediments and hence little net sediment accumulation. Thus, material being transported over the shelf is intercepted by the canyon and together with the material transported from the canyon head is accumulated in the middle part of the canyon. Radioisotope fluxes in the lower part of canyon, at water depths > 1500 m, are similar to values measured at comparable water depths located on the open adjacent slope, indicating that this part of the canyon is inactive on annual to decadal time scales. At longer time-scales, the sediments slowly and continuously accumulated at the middle canyon can be violently flushed towards the low canyon, as suggested by $^{210}Pb_{xs}$-depleted subsurface sediment layers observed at water depth > 2000 m inside the canyon.

The disconnection of the CFC from major sources of sediment delivery seems to limit its efficiency in particle transfer from coastal areas to the adjacent ocean basin. However, the middle part of CFC (water depth = 500–1500 m) acts as an efficient trap of particles laterally advected along the Aquitanian margin.

Acknowledgements

Crews of the R/V "Côte de la Manche" (CNRS-INSU) and engineers of Technical Department of INSU are sincerely acknowledged for their great help with sampling. We are grateful to the French FORCLIM Project (ANR-05-BLAN-02751) for the funding of the trap experiment on the Landes Plateau. Cruises were

supported respectively by the ANR FORCLIM and EC2CO BIOMIN programs. The acquisition of the low-background gamma detector was funded in part by the CNRS (LEBE-CYBER), the Aquitain Research council and the University of Bordeaux. A 3-year doctoral fellowship was provided to P. Duros by the Regional Council of Pays de la Loire. We wish to warmly thank the two anonymous reviewers for their pertinent comments and concrete contributions that helped improve the conceptual framework of the sedimentary activity in the CFC canyon.

References

Aller, R.C., Cochran, J.K., 1976. $^{234}Th/^{238}U$ disequilibrium in near-shore sediment: particle reworking and diagenetic timescales. Earth Planet. Sci. Lett. 29, 37–50.

Aller, R.C., DeMaster, D.J., 1984. Estimates of particle flux and reworking at the deep-sea floor using $^{234}Th/^{238}U$ disequilibrium. Earth Planet. Sci. Lett. 67, 308–318.

Antia, A.N., von Bodungen, B., Peinert, R., 1999. Particle fluxes across the mid-European continental margin. Deep-Sea Res. I 46 1999–2024.

Appleby, P.G., Oldfield, F., 1992. Application of lead-210 to sedimentation studies. In: Ivanovich, M., Harmon, R.S. (Eds.), Uranium-Series Disequilibrium: Applications to Earth, Marine, and Environmental Sciences. Clarendon Press, Oxford, pp. 731–778.

Beaufort, L., Heussner, S., 1999. Coccolithophorids on the continental slope of the Bay of Biscay: production, transport and contribution to mass fluxes. Deep-Sea Res. II 46, 2147–2174.

Bolliet, T., Jorissen, F.J., Schmidt, S., Howa, H., 2014. Benthic foraminifera from Capbreton Canyon revisited; faunal evolution after repetitive sediment disturbance. Deep-Sea Res. II 104, 319–334.

Bourillet, J.F., Zaragosi, S., Mulder, T., 2007. The French Atlantic margin and the deep sea submarine systems. Deep-sea turbidite systems on French margin. In: Mulder, T. (Ed.), Deep-Sea Turbidite Systems on French Margins: Geo-Marine Letters, SI 26; 2007, pp. 311–316.

Carpenter, R., Peterson, M.L., Bennett, J.T., 1982. ^{210}Pb-derived sediment accumulation and mixing rates for the Washington continental slope. Mar. Geol. 48, 135–164.

Carson, B., Baker, E.T., Hickey, B.M., Nittrouer, C.A., DeMaster, D.J., Thorbjarnarson, K.W., Snyder, G.W., 1986. Modern sedimentation dispersal and accumulation in Quinault submarine canyon: a summary. Mar. Geol. 71, 1–13.

Cochran, J.K., 1980. The flux of ^{226}Ra from deep-sea sediments. Earth Planet. Sci. Lett. 49, 381–392.

Cochran, J.K., McKibbin-Vaughan, T., Dornblaser, M.M., Hirschberg, D., Livingston, H.D., Buesseler, K.O., 1990. ^{210}Pb scavenging in the North Atlantic and North Pacific Oceans. Earth Planet. Sci. Lett. 97, 332–352.

Cremer, M., Orsolini, P., Ravenne, C., 1985. Cap-Ferret Fan, Atlantic Ocean. In: Bouma, A.H., Normark, W.R., Barnes, N.E. (Eds.), Submarine Fans and Related Turbidites Systems. Springer, New York, p. 113120.

Cunha, M.R., Paterson, G.L.J., Amaro, T., Blackbird, S., de Stigter, H.C., Ferreira, C., Glover, A., Hilário, A., Kiriakoulakis, K., Neal, L., Ravara, A., Rodrigues, C.F., Tiago, Á., Billett, D.S.M., 2011. Biodiversity of macrofaunal assemblages from three Portuguese submarine canyons (NE Atlantic). Deep-Sea Res. II 58, 2433–2447.

De Leo, F.C., Smith, C.R., Rowden, A.A., Bowden, D.A., Clark, M.R., 2010. Submarine canyons: hotspots of benthic biomass and productivity in the deep sea. Proc. Roy. Soc. Ser. B 277, 2783–2792.

de Stigter, H.C., Boer, W., de Jesus Mended, P.A., Thomsen, L., van der Bergh, G.D., van Weering, T.C.E., 2007. Recent sediment transport and deposition in the Nazaré Canyon, Portuguese continental margin. Mar. Geol. 246, 144–164.

de Stigter, H.C., Jesus, C.C., Boer, W., de Jesus Mendes, P.A., Richter, T.O., Costa, A., van Weering, T.C.E., 2011. Recent sediment transport and deposition in the Lisbon-Setubal and Cascais submarine canyons, Portuguese continental margin. Deep Sea Res. II 58, 2321–2344.

Duros, P., Fontanier, C., Metzger, E., Cesbron, F, Deflandre, B., Schmidt, S., Buscail, R., Zaragosi, S., Kerhervé, P., Jorissen, F.J., 2013. Live (stained) benthic foraminifera from the Cap-Ferret Canyon (Bay of Biscay, NE Atlantic): a comparison between the canyon axis and the surrounding areas. Deep-Sea Res. I. doi 10.1016/j.dsr.2013.01.004.

Duros, P., Fontanier, C., Cesbron, F., Zaragosi, S., Schmidt, S., Metzger, E., Jorissen, F. (submitted for publication). Taphonomical and biological impact on benthic foraminiferal thanatocoenoses from the Cap-Ferret Canyon area (NE Atlantic). Deep-Sea Res. II.

Durrieu de Madron, X., Castaing, P., Nyffeler, F., Courp, Th., 1999. Slope transport of suspended particulate matter on the Aquitanian margin of the Bay of Biscay. Deep-Sea Res. II 46, 2003–2027.

Gardner, W.D., 1989. Baltimore Canyon as a modern conduit of sediment to the deep sea. Deep-Sea Res. 36, 323–358.

Gaudin, M., 2006. Processus et enregistrements sédimentaires dans les canyons sous-marins Bourcart et de Capbreton durant le dernier cycle climatique. Unpublished Ph.D. Thesis, University of Bordeaux 1, 3122, 296 pp.

Gaudin, M., Mulder, T., Cirac, P., Berné, S., Imbert, P., 2006. Past and present sedimentary activity in the Capbreton Canyon, southern Bay of Biscay. In: Mulder, T. (Ed.), Deep-Sea Turbidite Systems on French Margins: Geo-Marine Letters, SI 26; 2006, pp. 331–346.

Harris, P.T., Whiteway, T., 2011. Global distribution of large submarine canyons: geomorphic differences between active and passive continental margins. Mar. Geol. 285, 69–86.

Heussner, S., Durrieu de Madron, X., Radakovitch, O., Beaufort, L., Biscaye, P.E., Carbonne, J., Delsaut, N., Etcheber, H., Monaco, A., 1999. Spatial and temporal patterns of downward particle fluxes on the continental slope of the Bay of Biscay (northeastern Atlantic). Deep-Sea Res. II 46, 2101–2146.

Huh, C.A., Liu, J.T., Lin, H.L., Xu, J.P., 2009. Tidal and flood signatures of settling particles in the Gaoping submarine canyon (SW Taiwan) revealed from radionuclide and flow measurements. Mar. Geol. 267, 8–17.

Hung, J.J., Lin, C.S., Chung, Y.C., Hung, G.W., Liu, W.S., 2003. Lateral fluxes of biogenic particles through the Mien-Hua canyon in the southern East China Sea slope. Cont. Shelf Res. 23, 935–955.

Hunter, W.R., Jamieson, A., Huvenne, V.A.I., Witte, 2013. Sediment community responses to marine vs. terrigenous organic matter in a submarine canyon. Biogeosciences 10, 67–80.

Jenner, K.A., Piper, D.J.W., Campbell, D.C., Mosher, D.C., 2007. Lithofacies and origin of late Quaternary mass transport deposits in submarine canyons, central Scotian Slope, Canada. Sedimentology 54, 19–38.

Jobe, Z.R., Lowe, D.R., Uchytil, S.J., 2011. Two fundamentally different types of submarine canyons along the continental margin of Equatorial Guinea. Mar. Petrol. Geol. 28, 843–860.

Kao, S.-J., Shiah, F.K., Wang, C.H., Liu, K.K., 2006. Efficient trapping of organic carbon in sediments on the continental margin with high fluvial sediment input off southwestern Taiwan. Cont. Shelf Res. 26, 2520–2537.

Kuhnt T., Howa H., Schmidt S., Marié L., Schielbel R., 2013. Flux dynamics of planktic foraminiferal tests in the south-eastern Bay of Biscay (Northeast Atlantic margin). J. Mar. Sys. ⟨/10.1016/j.jmarsys.2011.11.026⟩.

Legeleux, F., Reyss, J.L., Schmidt, S., 1994. Particle mixing rates in sediments of the North-East Tropical Atlantic: evidence from $^{210}Pb_{xs}$, ^{137}Cs, $^{228}Th_{xs}$, and $^{234}Th_{xs}$ downcore distribution. Earth Planet. Sci. Lett. 128, 545–562.

Maneux, E., Dumas, J., Clément, O., Etcheber, H., Charritton, X., Etchart, J., Veyssy, E., Rimmelin, P., 1999. Assessment of suspended matter input into the oceans by small mountainous coastal rivers: the case of the Bay of Biscay. C.R. Acad. Sci. Paris 329, 413–420.

Martín, J., Palanques, A., Vitorino, J., Oliveira, A., de Stigter, H., 2011. Near-bottom particulate matter dynamics in the Nazaré submarine canyon under calm and stormy conditions. Deep-Sea Res. II 58, 2388–2400.

Mas, V., Mulder, T., Dennielou, B., Schmidt, S., Khripounoff, A., Savoye, B., 2010. Multiscale spatio–temporal variability of sedimentary deposits in the Var Turbidite System (North-Western Mediterranean Sea). Mar. Geol. 275, 37–52.

McHugh, C.N., Ryan, W.B.F., Hecker, B., 1992. Contemporary sedimentary processes in the Monterey Canyon-fan system. Mar. Geol. 107, 35–50.

Muhammad, Z., Bentley, S.J., Febo, L.A., Droxler, A.W., Dickens, G.R., Peterson, L.C., Opdyke, B.N., 2008. Excess ^{210}Pb inventories and fluxes along the continental slope and basins of the Gulf of Papua. J. Geophys. Res. 113.

Mulder, T., Savoye, B., Piper, D.J.W., Syvitski, J.P.M., 1998. The Var submarine sedimentary system: understanding Holocene sediment delivery processes and their importance to the geological record. In: Stoker, M.S., Evans, D., Cramp, A. (Eds.), Geological Processes on Continental Margin: Sedimentation, Mass-Wasting and Stability, 129. Geological Society, London, pp. 145–166. (special publication).

Mulder, T., Weber, O., Anschutz, P., Jorissen, F.J., Jouanneau, J.M., 2001. A few months-old storm-generated turbidite deposited in the Capbreton Canyon (Bay of Biscay, SW France). Geo-Mar. Lett. 21, 149–156.

Mulder, T., Zaragosi, S., Garlan, T., Mavel, J., Cremer, M., Sottolichio, A., Senechal, N., Schmidt, S., 2012. Present deep-submarine canyons activity in the Bay of Biscay (NE Atlantic). Mar. Geol. 295, 113–127.

Mullenbach, B.L., Nittrouer, C.A., 2000. Rapid deposition of fluvial sediment in the Eel Canyon, northern California. Cont. Shelf Res. 20, 2191–2212.

Nittrouer, C.A., DeMaster, D.J., McKee, B.A., Cutshall, N.H., Larsen, I.L., 1984. The effect of sediment mixing on Pb-210 accumulation rates for the Washington continental shelf. Mar. Geol. 54, 201–221.

Ogston, A.S., Drexler, T.M., Puig, P., 2008. Sediment delivery, resuspension, and transport in two contrasting canyon environments in the southwest Gulf of Lions. Cont. Shelf Res. 28, 2000–2016.

Palanques, A., El Khatab, M., Puig, P., Masque, P., Sanchez-Cabeza, J.A., Isla, E., 2005. Downward particle fluxes in the Guadiaro submarine canyon depositional system (northwestern Alboran Sea), a river flood dominated system. Mar. Geol. 220, 23–40.

Palanques, A., Guillén, J., Puig, P., Durrieu de Madron, X., 2008. Storm-driven shelf-to-canyon suspended sediment transport at the southwestern Gulf of Lions. Cont. Shelf Res. 28, 1947–1956.

Palanques, A., Puig, P., Guillén, J., Durrieu de Madron, X., Latasa, M., Scharek, R., Martín, J., 2011. Effects of storm events on the shelf-to-basin sediment transport in the southwestern end of the Gulf of Lions (Northwestern Mediterranean). Nat. Hazards Earth Syst. Sci. 11, 843–850.

Pasqual, C., Lee, C., Goni, M., Tesi, T., Sanchez-Vidal, A., Calafat, A., Canals, M., Heussner, S., 2011. Use of organic biomarkers to trace the transport of marine and terrigenous organic matter through the southwestern canyons of the Gulf of Lion. Mar. Chem. 126, 1–12.

Pingree, R.D., Le Cann, B., 1995. Structure, strength and seasonality of the slope currents in the Bay of Biscay region. J. Mar. Biol. Assoc. UK 70, 857–885.

Puig, P., Ogston, A.S., Mullenbach, B.L., Nittrouer, C.A., Sternberg, R.W., 2003. Shelf-to-canyon sediment-transport processes on the Eel continental margin (northern California). Mar. Geol. 193, 129–149.

Puig, P., Palanques, A., Orange, D.L., Lastras, G., Canals, M., 2008. Dense shelf water cascades and sedimentary furrow formation in the Cap de Creus Canyon, northwestern Mediterranean Sea. Cont. Shelf Res. 28, 2017–2030.
Radakovitch, O., Heussner, S., 1999. Fluxes and budget of ^{210}Pb on the continental margin of the Bay of Biscay (northeastern Atlantic). Deep-Sea Res. II 46, 2175–2203.
Reid, G.S., Hamilton, D., 1990. A reconnaissance survey of the Whittard Sea Fan, southwestern Approaches, British Isles. Mar. Geol. 92, 69–86.
Reverdin, G., Marié, L., Lazure, P., d'Ovidio, F., Boutin, J., Testor, P., Martin, N., Lourenco, A., Gaillard, F., Lavin, A., Rodriguez, C., Somavilla, R., Mader, J., Rubio, A., Blouch, P., Rolland, J., Blouch, P., Rolland, J., Bozec, Y., Charria, G., Batifoulier, F., Dumas, F., Louazel, S., Chanut, J., 2013. Freshwater from the Bay of Biscay shelves in 2009. J. Mar. Sys. 109-110, S134–S143.
Robbins, J., Edgington, D.N., 1975. Determination of recent sedimentation rates in Lake Michigan using ^{210}Pb and ^{137}Cs. Geochim. Cosmochim. Acta 39, 285–304.
Ruch, P., Mirmand, M., Jouanneau, J.M., Latouche, C., 1993. Sediment budget and transfer of suspended sediment from Gironde Estuary to Cap-Ferret Canyon. Mar. Geol. 111, 109–119.
Sanchez-Cabeza, J.A., Ruiz-Fernández, A.C., 2012. ^{210}Pb sediment radiochronology: an integrated formulation and classification of dating models. Geochim. Cosmochim. Acta 82, 183–200.
Schmidt, S., Reyss, J.L., 1996. Radium as internal tracer of Mediterranean outflow water. J. Geophys. Res. 101, 3589–3596.
Schmidt, S., de Stigter, H.C., van Weering, T.C.E., 2001. Enhanced short-term sediment deposition within the Nazaré Canyon, North-East Atlantic. Mar. Geol. 173, 55–67.
Schmidt, S., van Weering, T.C.E., Reyss, J.L., van Beek, P., 2002. Seasonal deposition and reworking at the sediment-water interface on the north-western Iberian Margin. Prog. Oceanogr. 52, 331–348.
Schmidt, S., Howa, H., Mouret, A., Lombard, F., Anschutz, P., Labeyrie, L., 2009. Particle fluxes and recent sediment accumulation on the Aquitanian margin of Bay of Biscay. Cont. Shelf Res. 29, 1044–1052.
Schmidt, S., De Deckker, P., Etcheber, H., Caradec, S., 2010. Are the Murray Canyons Group offshore southern Australia still active for sediment transport? In: Bishop, P., Pillans, B. (Eds.), Australian Landscapes, Geological Society, London, pp. 43–45.
Shepard, F.P., Dill, R.F., 1966. Submarine Canyons and Other Sea Valleys. Rand McNally, Chicago p. 381.
Straub, K.M., Mohrig, D., 2009. Constructional canyons built by sheet-like turbidity currents: observations from offshore Brunei Darussalam. J. Sedim. Res. 79, 24–39.
Stefanescu, C., Morales-Nin, B., Massuti, E., 1994. Fish assemblages on the slope in the Catalan Sea (western Mediterranean): influence of a submarine canyon. J. Mar. Biol. Assoc. UK 74, 499–512.
Suykens, K., Schmidt, S., Delille, B., Harlay, J., Chou, L., De Bodt, C., Fagel, N, Borges, A.V., 2011. Benthic remineralization in the northwest European continental margin (northern Bay of Biscay). Cont. Shelf Res. 31, 644–658.
Tesi, T., Langone, L., Goñi, M.A., Turchetto, M., Miserocchi, S., Boldrin, A., 2008. Source and composition of organic matter in the Bari canyon (Italy): dense water cascading versus particulate export from the upper ocean. Deep-Sea Res. I 55, 813–831.
Van der Klooster, E, van Egmond, FM, Sonneveld, MPW, 2011. Mapping soil clay contents in Dutch marine districts using gamma-ray spectrometry. Eur. J. Soil Sci. 62, 743–753.
van Weering, T.C.E., Hall, I.R., de Stigter, H.C., McCave, I.N., Thomsen, L, 1998. Recent sediments, sediment accumulation and carbon burial at Goban Spur, N.W. European Continental Margin (47–50°N). Progr. Oceanogr. 42, 5–35.
van Weering, T.C.E., de Stigter, H.C., Boer, W., de Haas, H., de Stigter, H.C., Boer, W., de Haas, H., 2002. Recent sediment transport and accumulation on the NW Iberian margin. Progr. Oceanogr. 52, 349–371.
Vetter, E.W., 1994. Hotspots of benthic production. Nature 372, 47.
Zaragosi, S., Auffret, G.A., Faugères, J.C., Garlan, T., Pujol, C., Cortijo, E., 2000. Physiography and recent sediment distribution of the Celtic Deep-sea Fan, Bay of Biscay. Mar. Geol. 169, 207–237.